



HAL
open science

Discovery of N - β - 1 -Fucosyl Amides as High-Affinity Ligands for the *Pseudomonas aeruginosa* Lectin LecB

Patrycja Mala, Eike Siebs, Joscha Meiers, Katharina Rox, Annabelle Varrot, Anne Imberty, Alexander Titz

► **To cite this version:**

Patrycja Mala, Eike Siebs, Joscha Meiers, Katharina Rox, Annabelle Varrot, et al.. Discovery of N - β - 1 -Fucosyl Amides as High-Affinity Ligands for the *Pseudomonas aeruginosa* Lectin LecB. *Journal of Medicinal Chemistry*, 2022, 65 (20), pp.14180-14200. 10.1021/acs.jmedchem.2c01373 . hal-03834673

HAL Id: hal-03834673

<https://hal.science/hal-03834673>

Submitted on 30 Oct 2022

HAL is a multi-disciplinary open access archive for the deposit and dissemination of scientific research documents, whether they are published or not. The documents may come from teaching and research institutions in France or abroad, or from public or private research centers.

L'archive ouverte pluridisciplinaire **HAL**, est destinée au dépôt et à la diffusion de documents scientifiques de niveau recherche, publiés ou non, émanant des établissements d'enseignement et de recherche français ou étrangers, des laboratoires publics ou privés.

Discovery of *N*- β -L-Fucosyl Amides as High-Affinity Ligands for the *Pseudomonas aeruginosa* Lectin LecB

Patrycja Mała^{#1,2}, Eike Siebs^{#1,3,4}, Joscha Meiers^{1,3,4}, Katharina Rox^{4,5}, Annabelle Varrot⁶, Anne Imberty⁶, Alexander Titz^{1,3,4*}

¹Chemical Biology of Carbohydrates (CBCH), Helmholtz-Institute for Pharmaceutical Research Saarland (HIPS), Helmholtz Centre for Infection Research, 66123 Saarbrücken, Germany;

²Faculty of Chemistry, Adam Mickiewicz University, 61-614 Poznań, Poland;

³Department of Chemistry, Saarland University, 66123 Saarbrücken, Germany;

⁴Deutsches Zentrum für Infektionsforschung (DZIF), Standort Hannover-Braunschweig, Germany;

⁵Chemical Biology (CBIO), Helmholtz Centre for Infection Research, Braunschweig, Germany;

⁶Univ. Grenoble Alpes, CNRS, CERMAV, 38000 Grenoble, France.

#These authors contributed equally to this work.

*corresponding author e-mail: alexander.titz@helmholtz-hzi.de

Keywords: Lectin, carbohydrates, fucose, glycomimetics, LecB

Abstract

Pseudomonas aeruginosa is listed by the World Health Organization (WHO) as the most critical Gram-negative pathogen resisting antimicrobial treatment. It causes severe infections mainly in immuno-compromised or cystic fibrosis patients, which are difficult to treat due to its ability to form biofilms that protect the bacteria from antibiotics. One of the key players in bacterial adhesion to the host and biofilm formation is the lectin LecB, an extracellular protein that stabilizes the biofilm matrix. For the inhibition of LecB, we designed and synthesized a set of fucosyl amides, sulfonamides and thiourea derivatives. Then, we analyzed their binding to LecB in competitive and direct binding assays. We identified β -fucosyl amides as high-affinity ligands with unprecedented affinity for LecB in the two-digit nanomolar range. The molecules further showed good stability in murine and human blood plasma and hepatic metabolism, providing a basis for future development into antibacterial drugs. Finally, X-ray crystallography of an α - and a β -anomer of *N*-fucosyl amides in complex with LecB revealed the interactions responsible for the high affinity of the β -anomer at atomic level.

Introduction

Antimicrobial resistance is a rapidly developing threat to humanity.¹ The Gram-negative bacterium *P. aeruginosa* belongs to the problematic ESKAPE panel and is listed as the most critical drug-resistant bacterial pathogen by the WHO.² It is a threat to people with cystic fibrosis (CF) or chronic obstructive pulmonary disease (COPD) and to hospitalized immunocompromised patients.³ This bacterium can form biofilms which renders standard-of-care antibiotics orders of magnitude less effective.⁴ Moreover, many *P. aeruginosa* strains have become multi-drug resistant^{5,6} and several approaches to combat this problem are in the pipeline.³ An alternative strategy to antibiotics are antivirulence agents or pathoblockers, that instead of killing aim at disarming the bacteria in order to neutralize bacterial virulence and thereby provide protection to the host.^{3,7}

As the major resistance mechanism, the biofilm matrix hinders penetration of antibiotics and in addition, the embedded bacteria also reduce their metabolic activity rendering them persistent to treatment. One promising therapeutic option is thus to interfere with biofilm formation to restore antibiotic efficacy and also to provide access to the bacteria for the immune system. For establishing the biofilm, *P. aeruginosa* expresses two extracellular lectins LecA and LecB. Both proteins are crucial for initial cell adhesion. They are also essential constituents of the biofilm matrix^{8,9} and they establish interactions by binding to carbohydrate epitopes of the bacterial exopolysaccharides as well as to the bacterial and the host glycocalyx.^{10–12} The

sequences of LecA and LecB have been analyzed for various clinical and environmental isolates, demonstrating the lectins' functional conservation.^{13,14}

The binding of LecB to the biofilm matrix exopolysaccharide Psl¹¹ and its requirement for mature biofilm formation was demonstrated.⁹ Furthermore, LecA is involved in host cell invasion of *P. aeruginosa* by binding to the glycosphingolipid Gb3.¹⁵ In that process, LecA induces phosphorylation of the adaptor protein CrkII that mediates signaling across the host's plasma membrane which most likely assists the membrane engulfment.¹⁶ Infection experiments using *lecA* or *lecB* knockout strains revealed improved lung bacterial clearance in mice and better epithelial wound healing when compared to the corresponding wildtype bacteria.^{12,17}

A study on cystic fibrosis patients with chronic *P. aeruginosa* infections showed that inhalation of a L-fucose/ D-galactose solution reduced the amount of bacteria in sputum.¹⁸ In another study on *P. aeruginosa* lung infected mice, it could be demonstrated that administration of carbohydrates in combinations with antibiotics reduced the bacterial burden more efficiently than single treatments of antibiotics.¹⁹ Therefore, the synthesis of LecA and LecB inhibitors as novel anti-infectives is an active field of research.^{3,20,21}

LecA forms homotetramers and binds to D-galactosides *via* a calcium ion in its carbohydrate binding site.²² Several monovalent galactosides were synthesized as LecA inhibitors reaching moderate binding in the micromolar range.^{23–25} In contrast, divalent galactoside inhibitors with simultaneous binding to two adjacent carbohydrate binding sites of the LecA tetramer gave low nanomolar inhibitors.^{20,26–28} Novel concepts were also reported such as the development of covalent lectin inhibitors²⁹, addressing a subpocket between the two adjacent carbohydrate binding sites³⁰, or the development of non-carbohydrate glycomimetics^{31,32}.

LecB also forms homotetramers and possesses two calcium ions per carbohydrate binding site mediating binding to its fucoside or mannoside ligands.³³ The affinity of fucosides is increased compared to mannosides due to an additional lipophilic interaction of the fucose C6 methyl group with the protein at Thr45, resulting in sub-micromolar binding (**Figure 1A**, K_d of Me- α -L-Fuc = 0.43 μ M³⁴, K_d of Me- α -D-Man = 71 μ M³⁴). Furthermore, it was demonstrated that the CH₂OH group of mannosides adopts a sterically hindered position when bound to LecB.³⁵ However, the co-crystal structure of fucose in complex with LecB³³ revealed a subpocket next to the anomeric center that was subsequently addressed in our program for LecB inhibitors (**Figure 1A**, compound II).^{36–39} A small cleft between the carbohydrate binding site and said subpocket is surrounded by amino acids Ser22 and Asp96. The subpocket itself differs slightly between the two *P. aeruginosa* strains.¹³

Consequently, we have designed fucose-mannose hybrid glycomimetics^{35,36,40} combining the properties of our first set of D-mannose-derived inhibitors³⁷ with L-fucose resulting in sub-micromolar affinities (K_d (PAO1) (**I**) = 0.83 μ M⁴⁰, K_d (PA14) (**I**) = 0.29 μ M⁴⁰, **Figure 1B**), oral bioavailability in mice and good antibiofilm activity *in vitro*. Our initial mannosyl amides and sulfonamides as well as fucose-mannose hybrid molecules targeted this subpocket and the interactions could be explained on the basis of several X-ray LecB structures for both strains.^{36,37,40} We demonstrated that the mannose sulfonamides inhibited LecB better than the corresponding amides (IC_{50} (PAO1) (**III**) = 110 μ M, IC_{50} (PA14) (**III**) = 42 μ M, IC_{50} (PAO1) (**IV**) = 16 μ M, IC_{50} (PA14) (**IV**) = 3.3 μ M).^{36,37} Due to the different geometry in the sulfonamide moiety, these molecules can circumvent a steric clash of the amides with Ser97 on LecB_{PA14}.⁴⁰ However, the fucose-mannose hybrid amides were as active as the mannose sulfonamides (IC_{50} (PAO1) (**V**) = 8.7 μ M, IC_{50} (PA14) (**V**) = 3.5 μ M) due to hydrophobic interactions of their methyl groups (C6) with Thr45.⁴⁰ Shifting the amide/sulfonamide linker function further towards this subpocket by using an elongated heptose derivative resulted in a loss in affinity for LecB_{PAO1} ($IC_{50} \geq 82 \mu$ M).³⁸

In the present work, we further assessed the positioning and nature of the linking unit between the carbohydrate and the pharmacophore targeting the additional subpocket in LecB. To this end, we shortened the linking function in those molecules by removing a methylene group and combined the fucose pharmacophore with amide and sulfonamide functions, and furthermore, replaced the previously reported linkers in the hybrid-type molecules with thioureas.

Results and Discussion

Design of Fucosyl Amides and Sulfonamides, Fucosylmethyl Thioureas

To study the influence of the linking units between fucose and aromatic pharmacophores targeting the subpocket in LecB, we replaced the known amide and sulfonamide linkers of previous hybrid-type molecules **I** and **V**. First, we modified the chemical nature of the linker and introduced thioureas providing hydrogen-bond donor/acceptor properties resulting in molecules such as **11c** (**Figure 1C**) with altered geometry of the linking unit and elongation. Then, we shortened the molecules into analogs devoid of the methylene group in compounds **I** and **V** and designed *N*-fucosides of amides **4** and sulfonamides **8** to assess hydrogen bond formation with the amino acids such as Ser22 (**Figure S1**).

These molecules were first docked *in silico* into LecB. For fucosylmethyl *p*-tolylthiourea (**11c**), the carbohydrate moiety superimposes with fucose bound to LecB (**Figure S1**), while the thiourea forms hydrogen bonds with the backbone of Asp96 and with its sidechain. Interestingly,

the software docked the thiourea function in its tautomeric thiol form, although the thione is dominating in aqueous solutions.⁴¹ The docked binding pose of β -fucosyl benzamide (**4a**) showed again an identical orientation of the fucose, while its amide serves as hydrogen bond acceptor for the sidechain of Ser22. In addition, the aromatic ring forms lipophilic contacts with Gly24 and Val69 of the adjacent pocket (**Figure S1**).

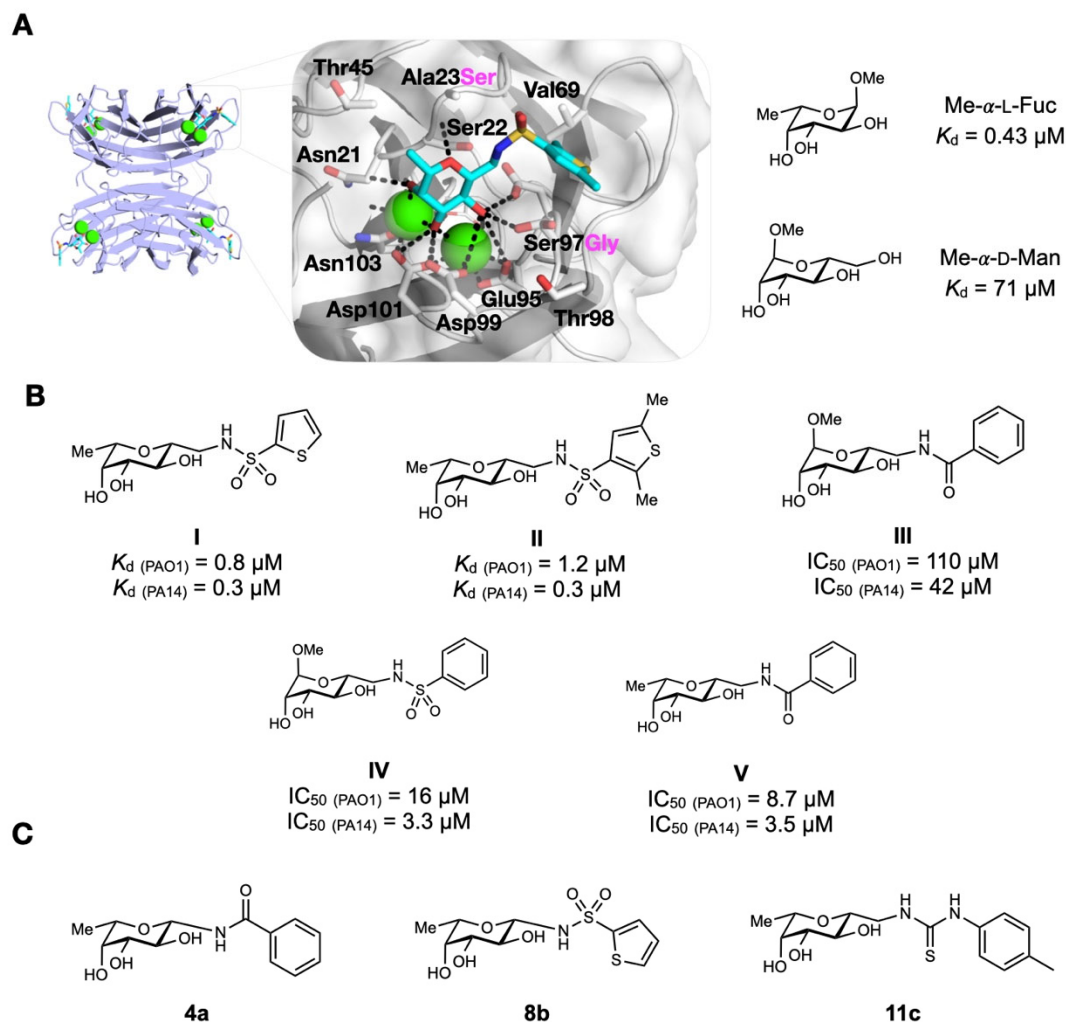


Figure 1: **A**) Crystal structure of LecB_{PA14} in complex with hybrid **II** (pdb: 5MAZ⁴⁰) with overall tetramer and zoom into the carbohydrate binding site (green spheres: calcium ions, red spheres: waters, red: oxygens, blue: nitrogen, pink: amino acid variations in LecB_{PAO1}); **B**) Previous low-molecular weight LecB inhibitors **I**³⁶, **II**, **V**⁴⁰, and **III–IV**^{36,37}. **C**) Designed LecB inhibitors *N*-fucosyl amides (e.g. **4a**), *N*-fucosyl sulfonamides (e.g. **8b**) and fucosylmethyl thioureas (e.g. **11c**) for this work.

Synthesis of Amides, Sulfonamides and Thioureas

β -Fucosyl amides were obtained in a three-step synthesis from fucose tetraacetate **1** (**Scheme 1**). Transformation of the tetraacetate into azide **2** was achieved in good yield (77%). This azide was further converted in a STAUDINGER reduction followed by acylation with acyl chlorides to the

corresponding protected β -fucosyl amides **3a–n** in yields of 12–71%. The target amides **4a–n** were then obtained after deacetylation under ZEMPLÉN conditions (47–99%). Furthermore, one α -fucosyl amide, benzamide **6**, was also synthesized to serve as a control molecule. **6** was obtained over two steps commencing from azide **2** by an activation with triphenylphosphine under reflux to form the α -oxazoline intermediate, which was coupled with a thiopyridyl ester of benzoic acid using DE SHONG⁴² conditions to form the protected α -fucosyl amide **5** in 27% yield. The latter compound was finally deprotected to give the α -anomer **6** in 98% yield.

In contrast, the fucosyl sulfonamides **8a–b** were synthesized by *N*-glycosylation of the respective sulfonamides. To this end, the sulfonamide acceptors were treated with tetraacetate **1** as donor under Lewis acid catalysis and the pure β -glycosides **7a–b** were obtained in good yields. Unfortunately, the subsequent deprotection step using sodium methoxide inevitably resulted in anomerization and the test compounds were obtained as anomeric mixtures.

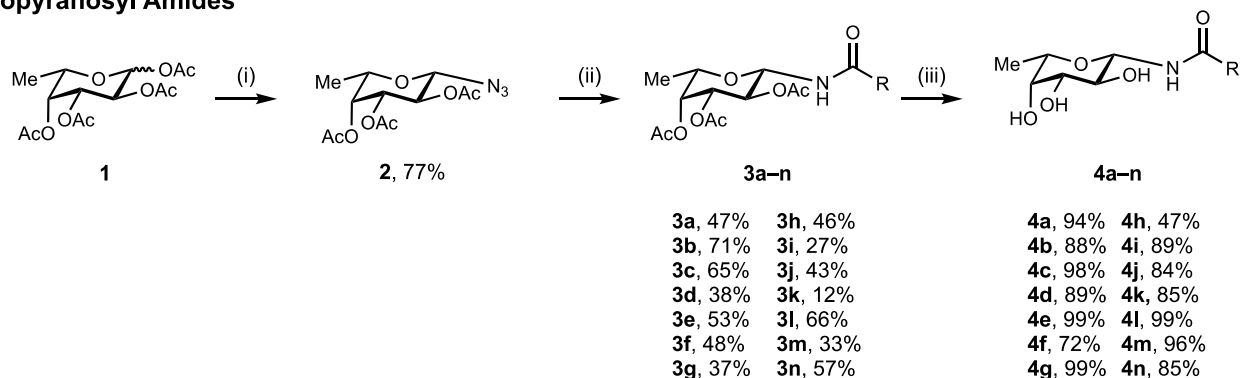
The β -fucosylmethyl thioureas **11c–e, o, p** were obtained in a three step synthesis from L-fucose. Optimized HENRY⁴³ reaction conditions of fucose and nitromethane were used to obtain condensation product **9**. After reduction of nitro **9** to the amine **10**, the latter was reacted with various isothiocyanates to give the thioureas **11c–e, o, p** in good yields (71–80%).

In total, 22 fucose derivatives were synthesized (**Scheme 1**), among which are 14 β -fucosyl amides, one α -fucosyl amide, two fucosyl sulfonamides obtained as α/β mixtures, and five β -fucosylmethyl thioureas.

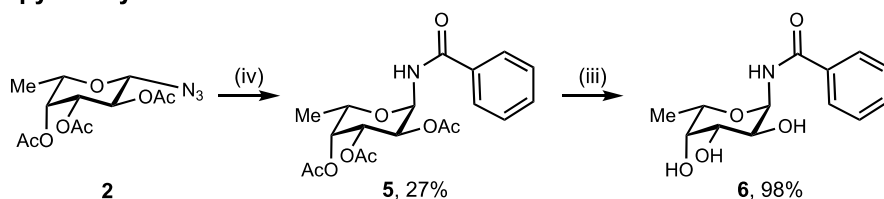
Evaluation of LecB Binding in Biophysical Assays

All ligands were then tested in a competitive binding assay³⁷ based on fluorescence polarization for dose-dependent inhibition of LecB_{PAO1}. Due to obtained high affinities of the β -fucosyl amides, the assay was slightly modified and a lower LecB concentrations of 75 nM was used (**Table 1**). Therefore, the obtained data for L-fucose was also slightly lower with an $IC_{50} = 1.35 \pm 0.04 \mu\text{M}$ compared to the reported value of $2.74 \mu\text{M}$ ³⁷.

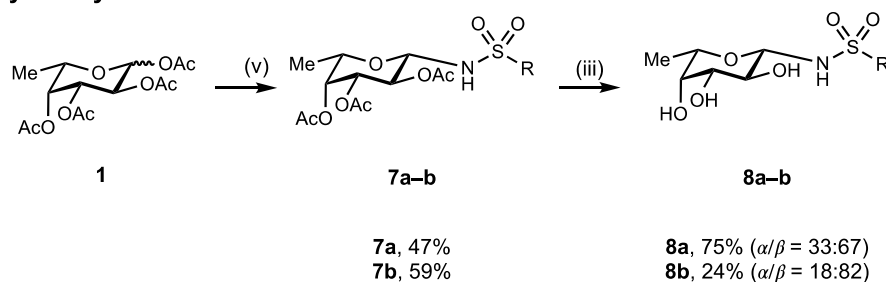
β -Fucopyranosyl Amides



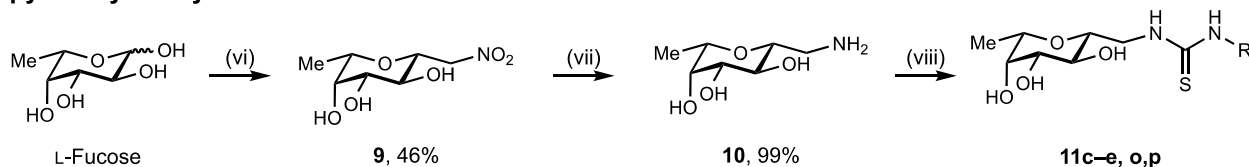
α -Fucopyranosyl Amide



Fucopyranosyl Sulfonamides



β -Fucopyranosylmethyl Thioureas



| | |
|--|--|
| R = a , Ph- | i , <i>m</i> Ph-C ₆ H ₄ - |
| b , 2-Thiophenyl- | j , Me- |
| c , <i>p</i> CH ₃ -C ₆ H ₄ - | k , (CH ₃) ₂ CH- |
| d , <i>p</i> MeO-C ₆ H ₄ - | l , (<i>E</i>)-PhCH=CH- |
| e , <i>p</i> NO ₂ -C ₆ H ₄ - | m , 2-Naphthyl- |
| f , <i>p</i> Cl-C ₆ H ₄ - | n , 2-Furanyl- |
| g , <i>p</i> CF ₃ -C ₆ H ₄ - | o , <i>p</i> Et-C ₆ H ₄ - |
| h , <i>m</i> CH ₃ -C ₆ H ₄ - | p , <i>p</i> F-C ₆ H ₄ - |

| |
|------------------|
| 11c , 71% |
| 11d , 79% |
| 11e , 71% |
| 11o , 74% |
| 11p , 80% |

Scheme 1: Synthesis of LecB ligands β -fucosyl amides (**4a-n**), α -fucosyl amide (**6**), fucosyl sulfonamides (**8a-b**) and β -fucopyranosylmethyl thioureas (**11c,d,e,o,p**). Reagents and conditions: (i) Me₃SiN₃, SnCl₄, CH₂Cl₂, 25 °C, 1.5 h; (ii) RCOCl, PPh₃, Et₃N, CH₂Cl₂, 0–25 °C, o.n.; (iii) NaOMe, MeOH, -25 to -15 °C or 0 °C, o.n. or 1.5 h; (iv) 1. PPh₃, MeNO₂, 4 Å molecular sieves, reflux, 24 h; 2. S-(pyridin-2-yl) benzothioate, CuCl₂·H₂O; (v) phenylsulfonamide or thiophene-2-yl-sulfonamide, BF₃·OEt₂, MeCN, 25 °C, 24 h; (vi) 1. MeNO₂, NaOMe (cat.), DMSO, 25 °C, 6 h; 2. HCl (1 M, pH = 4), H₂O, reflux, o.n.; (vii) Pt/C, H₂, MeOH, 25 °C, 48 h; (viii) isothiocyanates, MeOH, 0–25 °C, o.n.

In this assay, all tested β -fucosyl amides inhibited LecB in the nanomolar range. Acetamide **4j** showed the weakest inhibition among the series giving an IC_{50} of 902 ± 69 nM. The affinity increased among this compound class when the acetamide was replaced with larger substituents: replacing its methyl with aromatic rings such as 2-furanosyl (IC_{50} (**11**) = 272 ± 26 nM), 2-thiophenyl (IC_{50} (**4b**) = 122 ± 21 nM) or a phenyl ring increased the affinity towards LecB up to tenfold into the two-digit nanomolar range (IC_{50} (**4a**) = 88 ± 12 nM), which rendered fucosyl benzamide (**4a**) 15-fold more potent than L-fucose. Introducing electron-donating substituents on the phenyl ring (e.g. in **4c**, **4d**, **4f**, and **4h**) had a negligible effect on affinity, whereas the strongly electron-withdrawing substituents in **4e** and **4g** reduced the affinity by a factor 2. Extension of the ring system into a naphthyl (IC_{50} (**4m**) = 92 ± 13 nM) or a biphenyl (IC_{50} (**4i**) = 85 ± 16 nM) residue resulted in similarly high affinity as the benzamide **4a**. However, changing the configuration at the anomeric center from β -glycoside **4a** to its isomeric α -anomer **6** resulted in a 26-fold drop in affinity (IC_{50} (**6**) = 2324 ± 432 nM).

The fucosyl sulfonamides **8a** and **8b** were tested as anomeric mixtures and showed an affinity comparable to L-fucose (IC_{50} (**8a**) = 1496 ± 512 nM and IC_{50} (**8b**) = 1144 ± 247 nM). Since the β -anomer was the major anomer present in both cases (67% and 82%), we assigned a reduced LecB binding potency compared to the synthesized fucosyl analogs. When comparing these results to our previous β -fucosylmethyl sulfonamides for LecB_{PAO1} (IC_{50} = 0.97–1.80 μ M³⁶) we conclude a comparable activity of the sulfonamides independent of the presence of the methylene group, e.g. 2-thiophene **8b** lacking the methylene group is only slightly more active (factor 1.6) than its β -fucosylmethyl homolog (IC_{50} = 1.8 μ M⁴⁰).

The β -fucosylmethyl thioureas were also tested and proved 100-fold less active than the best carboxamides reported here (IC_{50} (**11c–e**, **11o**, **11p**) = 7.3–8.8 μ M). We observed a strong decrease in affinity of the thioureas compared to the previously reported sulfonamides **I** or **II**, although they were as potent as the fucosylmethyl carboxamides **V**.

The strong decrease in affinity for LecB observed here between the very active fucosyl amides and the less active sulfonamides could possibly result from two factors. First, the increased acidity of the sulfonamides compared to the carboxamides could impact their hydrogen-bonding properties. Second, the geometry of the substituents of an amide or a sulfonamide differ from planar trans to staggered gauche, which results in an altered orientation of the linked pharmacophores.

To validate the high affinity of the described LecB inhibitors in an orthogonal assay, we analyzed the two anomers of fucosyl benzamides, α -**6** and β -**4a**, by isothermal titration calorimetry (

Table 2). The K_d of β -fucosyl amide **4a** obtained by ITC was 195 ± 97 nM, and thus somewhat higher than the IC_{50} of 88 ± 12 nM obtained in the competitive binding assay. The binding enthalpy of $\Delta H = -29.4 \pm 1.3$ kJ mol⁻¹ was similar to the one reported for L-fucose ($\Delta H = -31.2$ kJ mol⁻¹⁴⁴), but the favorable entropic contribution $T\Delta S = 9.2$ kJ mol⁻¹ was much higher (L-Fuc = 0.3 kJ mol⁻¹⁴⁴) explaining the increase in binding affinity. α -Fucosyl benzamide (**6**) showed a K_d of 2.3 ± 0.4 μ M corresponding to the one previously reported for other types of α -fucosyl amides and LecB binding ($K_d = 1.2$ – 2.1 μ M⁴⁵). The enthalpy of LecB-binding of the α -anomer **6** ($\Delta H = -28.0$ kJ mol⁻¹) was nearly identical to the one observed for the β -anomer, while the entropic contribution was much lower for the α -anomer ($T\Delta S = 4.2$ kJ mol⁻¹). In general, α -linked substituents at the anomeric center of fucose point towards the solvent when bound to LecB, while β -linked substituents are oriented towards the protein surface, and thus the observed difference in binding entropy possibly resulted from displaced protein-bound water molecules for β -benzamide **4**. Favorable entropy of binding is very unusual in protein-carbohydrate interaction, and optimizing this thermodynamic contribution appears here as a valuable strategy.

Table 1: Inhibition of LecB_{PAO1} by fucosyl amides, sulfonamides and fucosylmethyl thioureas in a competitive binding assay²³. IC_{50} s and std. dev. determined from three independent experiments.

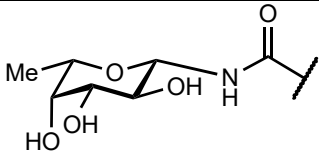
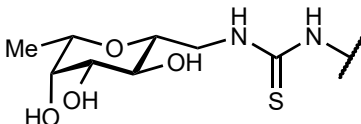
| No. | Structure | IC_{50} [nM] | No. | Structure | IC_{50} [nM] |
|------------|--|--|------------|---|--|
| | | | |  | |
| 4a | Ph- | 88 ± 12 | 4h | <i>m</i> CH ₃ -C ₆ H ₄ - | 120 ± 13 |
| 4b | 2-Thiophenyl- | 122 ± 21 | 4i | <i>m</i> Ph-C ₆ H ₄ - | 85 ± 16 |
| 4c | <i>p</i> CH ₃ -C ₆ H ₄ - | 110 ± 17 | 4j | CH ₃ - | 902 ± 69 |
| 4d | <i>p</i> CH ₃ O-C ₆ H ₄ - | 138 ± 20 | 4k | (CH ₃) ₂ CH- | 155 ± 18 |
| 4e | <i>p</i> NO ₂ -C ₆ H ₄ - | 204 ± 44 | 4l | (<i>E</i>)-PhCH=CH- | 302 ± 43 |
| 4f | <i>p</i> Cl-C ₆ H ₄ - | 130 ± 19 | 4m | 2-Naphthyl- | 92 ± 13 |
| 4g | <i>p</i> CF ₃ -C ₆ H ₄ - | 211 ± 41 | 4n | 2-Furanyl- | 272 ± 26 |
| 6 | α -Fucosyl benzamide | 2324 ± 432 | | | |
| 8a | Fucosyl benzene-sulfonamide | 1496 ± 512 ($\alpha/\beta = 33:67$) | 8b | Fucosyl thiophene-2-sulfonamide | 1144 ± 247 ($\alpha/\beta = 18:82$) |
| | | | |  | |
| 11c | <i>p</i> CH ₃ -C ₆ H ₄ - | 7387 ± 473 | 11o | <i>p</i> CH ₃ CH ₂ -C ₆ H ₄ - | 8112 ± 374 |
| 11d | <i>p</i> CH ₃ O-C ₆ H ₄ - | 7658 ± 288 | 11p | <i>p</i> F-C ₆ H ₄ - | 8831 ± 103 |

Table 2: Isothermal titration calorimetry of LecB with fucosyl benzamides β -**4a** and α -**6**; means and std. dev. were calculated from three independent titrations.

| Compound | ΔG [kJ mol ⁻¹] | K_d [nM] | n | ΔH [kJ mol ⁻¹] | $T\Delta S$ [kJ mol ⁻¹] |
|-----------|---------------------------------------|----------------|---------------|---------------------------------------|--|
| 4a | -38.6 | 195 ± 97 | 1.0 ± 0.1 | -29.4 ± 1.3 | 9.2 ± 0.4 |
| 6 | -32.2 | 2310 ± 350 | 0.9 ± 0.1 | -28.0 ± 1.7 | 4.2 ± 1.3 |

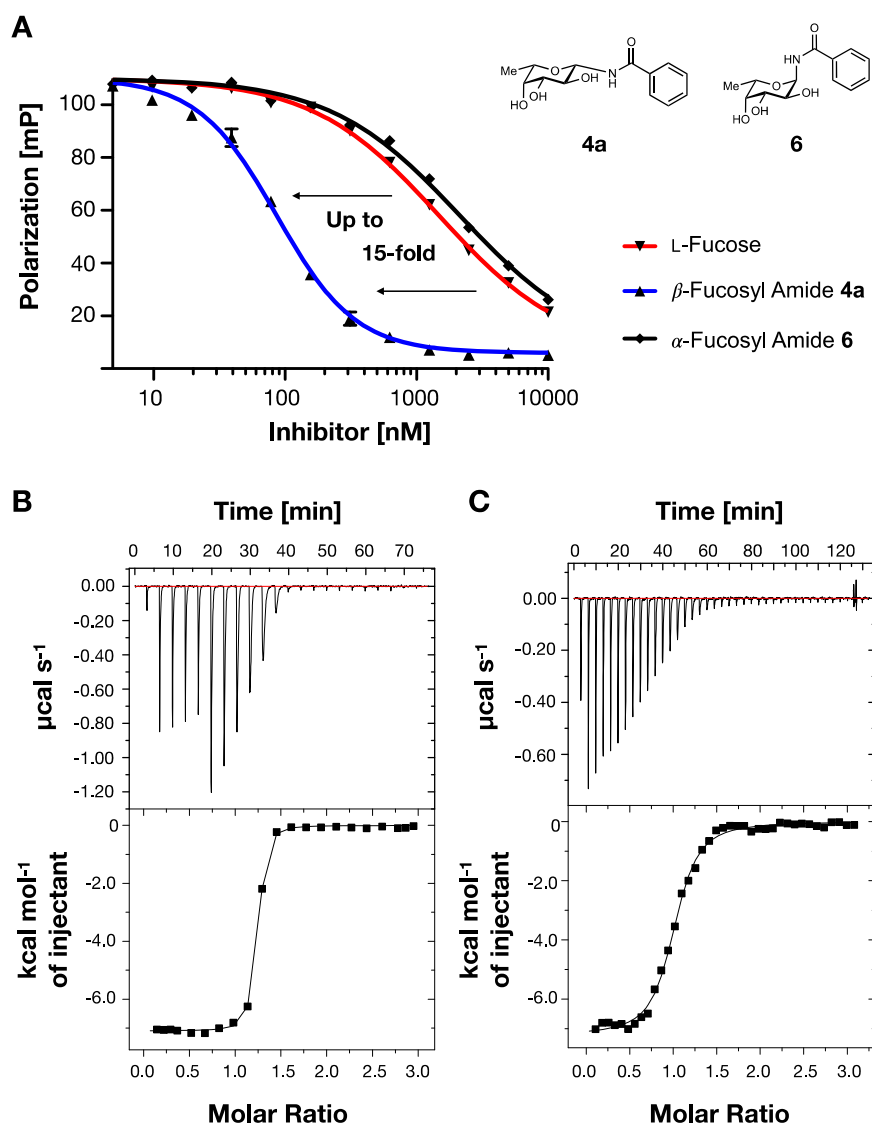


Figure 2: Biophysical analysis of fucosyl benzamides β -**4a** and α -**6** with LecB_{PAO1}: **A)** competitive binding assay based on fluorescence polarization shows a 15-fold increase of LecB inhibition for β -**4a** compared to its α -anomer **6**; **B)** isothermal titration calorimetry of β -fucosyl benzamide **4a** and of **C)** α -fucosyl benzamide **6** against LecB.

Both experiments show one respective titration of each fucosyl benzamide from one of the independent replicates, for **A** error bars correspond to those from technical triplicates of one independent replicate.

X-Ray Crystallography of α - and β -Fucosyl Amides in Complex with LecB

To analyze the interactions of the fucosyl amides at the atomic level, we co-crystallized compounds **4a**, **4i** and **6** with LecB_{PAO1}. Co-crystals were obtained for all compounds, but **4a** in complex with LecB diffracted to lower resolution. One dataset was collected for β -benzamide **4a** in complex with LecB and was solved at 2.5 Å resolution with two tetramers in the asymmetric unit. The electron density was poor for one of the tetramers and in some binding sites and not always well defined for the aglycon, so we decided not to refine it. The datasets obtained for β -biphenyl **4i** and α -benzamide **6** in complex with LecB were of high quality and the structures were solved at high resolution (**4i**: 1.55 Å, **6**: 1.50 Å) (**Figure 3**, **Table S4** for data quality). In both cases, the four carbohydrate binding sites of LecB were occupied by the ligands **4i** or **6**, and the fucose moiety of both ligands was firmly bound to the calcium-ions inside the carbohydrate binding site as reported previously for the fucose/LecB complex (pdb: 1GZT³³). In both ligands, the three hydroxy groups OH2, OH3 and OH4 bind to the calcium-ions and their C6 methyl group interacts with Thr45 and Ser23 *via* hydrophobic contacts (**Figure S2** and **S3** for individual protomers).

In the complex of α -fucosyl benzamide **6** (**Figure 3A**, **Figure S2**), the amide nitrogen points away from the surface of the protein and is integrated in the hydrate layer where it loosely binds to Thr98(NH) *via* one water molecule. Its carbonyl oxygen atom points towards the binding site and forms one hydrogen bond with Ser23 (2.47 – 3.25 Å). Additionally, a hydrogen bond *via* a water to Asp96 can be observed. The aromatic ring of the benzamide is rotated out of the plane of the amide bond. Its orientation depends on a crystal contact based on an edge-to-face interaction with another benzamide. Further, the benzamide ring forms loose lipophilic interactions with Gly97 (3.76 Å – 4.76 Å), that slightly depend on the rotation of the aromatic ring. Thus, the aromatic ring of α -fucosyl benzamide **6** only weakly contributes to the compounds' binding affinity towards LecB.

In the LecB complex of β -fucosyl biphenylamide **4i** (**Figure 3C**, **Figure S3**), the amide function occupies similar orientations in protomers B–D and differs slightly in protomer A. In the latter, the amide NH of **4i** serves as a hydrogen bond donor for Ser22(OH) that makes an ion-dipole interaction with Asp96(COO⁻). In protomers B–D there is a rotation of the carbonyl oxygen by approximately 60°. This allows the carbonyl oxygen to establish a hydrogen bond with Ser23(OH) facing toward the binding site (**Figure 3C**). The rotation further brings the NH in a dipole-ion interaction with Asp96, which could be an explanation for the high binding affinity of

the β -fucosyl amides. The directly attached phenyl ring forms lipophilic contacts with Gly24 and Val69. The distal ring is largely solvent exposed but also forms hydrophobic contacts with Asn70. This rather small additional contact area could explain the only very small affinity increase of biphenyl **4i** compared to the benzamide **4a** in the competitive binding assay.

To better understand the high affinity of fucosyl biphenylamide **4i**, we compared the two co-crystal structures of *manno*-cinnamide **S1** (pdb: 5A3O, $K_d = 18.5 \mu\text{M}$ against LecB_{PAO1}³⁹) or fucose-mannose hybrid **II** (pdb: 5MAZ, LecB_{PA14}, $K_d = 0.8 \pm 0.1 \mu\text{M}$ against LecB_{PAO1}³⁶) with biphenyl fucosylamide **4i** in complex with LecB_{PAO1} (**Figure S4**).

Superimposition of the complexes LecB_{PAO1}-**4i** and LecB_{PA14}-**S1** clearly shows the effect of the additional methylene group of **S1**. The amide NH of **4i** points in between Ser22 and Asp96 to form a hydrogen bond or dipole-ion interaction. On the other hand, the NH of **S1** is shifted by the methylene group and points beyond the carboxylic acid of Asp96 (**Figure S4**), therefore unable to neither form a hydrogen bond with Ser22, nor an efficient dipole-ion interaction with Asp96.

Also, for the fucose-mannose hybrid **II** the additional CH₂-spacer prevents an interaction of the sulfonamide NH with Ser22 and Asp96 (**Figure S5**). But in contrast to the amides, the nitrogen atom in the sulfonamide function is sp³ hybridized resulting in a conformationally distinct and more flexible linker that enables lipophilic interactions of the thiophene residue with Ser97, Gly24, Val69 and the CH₂ of Asp96, while the large biphenyl residues of **4i** point away from this shallow binding pocket. Interestingly, this orientation of **4i** is in alignment with the previously observed binding pose of **II** with crystal-contacts. The superimposition of **4i** and **II** suggests that introduction of a CH₂-linker next to the carbonyl of the amide functionality of **4i** could allow a certain flexibility of the aromatic substituent and perhaps restore the lipophilic interactions in **4i** as observed for dimethylthiophene **II**.

In summary, β -fucosyl biphenylamide **4i** aligns optimally with the surface of LecB because its amide nitrogen atom is ideally positioned to form a hydrogen bond with Ser22 or an ion-dipole interaction with Asp96, its amide carbonyl oxygen interacts with Ser23 and its proximal phenyl ring forms hydrophobic interactions in the adjacent pocket with Gly24 and Val69.

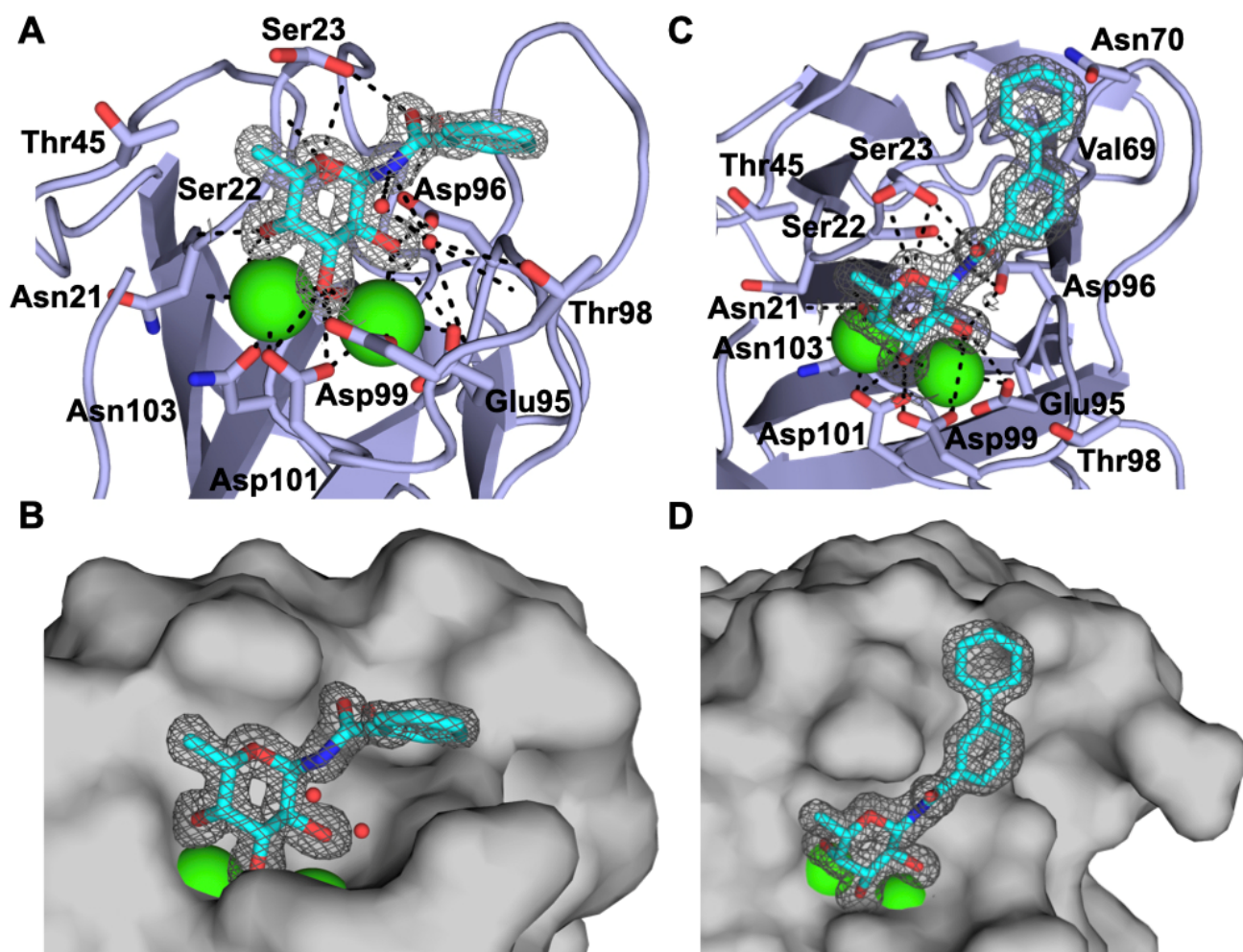


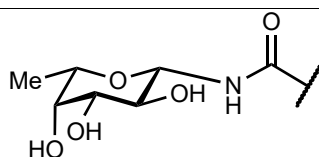
Figure 3: Co-crystal structures of α -fucosyl amide **6** (A, B) and β -fucosyl amide **4i** (C, D) in complex with LecB (pdb: 8AIY for **4i**, 8AIJ for **6**). Electron density is displayed at 1σ , ligands and amino acid residues in the binding site are shown as sticks, water molecules in red and Ca^{2+} -ions as green spheres. Dashed lines indicate hydrogen-bonding interactions of the specific ligand with the protein.

Metabolic Stability, Plasma Protein Binding, and Cytotoxicity

Next, we evaluated the compounds' metabolic stability using murine/human plasma and liver microsomes and analyzed their plasma protein binding (PPB) capacity (Table 3 and Table 4). In mouse plasma, seven out of 15 compounds showed good stability with half-lives between 85–145 min and 6 further compounds were fully stable: α -fucosyl benzamide (**6**), simple and aromatic β -fucosyl amides (**4b**, **4d**, **4k**, **4g**) and sulfonamide **8a**. Only compound **4f** with a *para*-chlorophenyl was less stable ($t_{1/2} = 23$ min). In human plasma, all compounds were very stable except fucosyl sulfonamide **8b** that degraded slowly ($t_{1/2} = 112$ min). Exceptions were acetamide **4j** and 2-furanoyl amide **4n** which were not detectable in human and murine plasma, suggesting fast degradation.

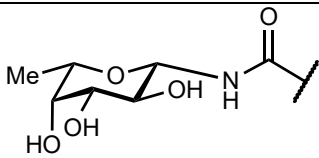
For mouse plasma, the lowest protein binding of 21% was obtained for isopropyl amide **4k**. Bulky β -fucosyl amide **4i** as well as 2-thiophenyl sulfonamide **8b** showed 100% binding, while other fucosyl amides showed PPB between 24–76%. *meta*-Methylbenzamide **4h** showed only 45% binding in mouse plasma compared to its *para*-isomer **4c** with non-detectable binding due to degradation processes in mouse plasma. In human plasma, most of the compounds showed a similar binding profile as in mouse plasma. However, especially **8b** exhibited differences: whereas **8b** showed much lower binding in human plasma, full binding in mouse plasma was observed. For compound **8b** these differences might be an artefact as **8b** was less stable in plasma *per se*, with better signals in human plasma. Biphenyl amide **4i** exhibited the highest plasma protein binding in both species compared to all other tested fucosyl amides.

Table 3: Mouse & human plasma stability and plasma protein binding of α -/ β -fucosyl amides and sulfonamides.

| No. | Structure | Plasma | | PPB | |
|-----------|---|-----------------------------|-----------------------------|--------------|--------------|
| | | Mouse $t_{1/2}$ [min] | Human $t_{1/2}$ [min] | Mouse [%] | Human [%] |
| |  | | | | |
| 4a | Ph- | n.d. | n.d. | 38 ± 5 | 49 ± 16 |
| 4b | 2-Thiophenyl- | stable | stable | 28 ± 10 | 70 ± 26 |
| 4c | <i>p</i> CH ₃ -C ₆ H ₄ - | 130 | stable | n.d. | 31 ± 9 |
| 4d | <i>p</i> CH ₃ O-C ₆ H ₄ - | stable | stable | 36 ± 14 | 12 ± 3 |
| 4e | <i>p</i> NO ₂ -C ₆ H ₄ - | 144 | stable | 46 ± 3 | 57 ± 16 |
| 4f | <i>p</i> Cl-C ₆ H ₄ - | 24 | stable | n.d. | 55 ± 18 |
| 4g | <i>p</i> CF ₃ -C ₆ H ₄ - | stable | stable | 58 ± 19 | 43 ± 29 |
| 4h | <i>m</i> CH ₃ -C ₆ H ₄ - | 85 | stable | 45 ± 20 | 35 ± 14 |
| 4i | <i>m</i> Ph-C ₆ H ₄ - | 119 | stable | 100 ± 0 | 90 ± 0 |
| 4j | Me | n.d. | n.d. | - | - |
| 4k | (CH ₃) ₂ CH- | stable | 207 | 21 ± 13 | 12 ± 9 |
| 4l | (<i>E</i>)-PhCH=CH- | 145 | stable | 18 ± 6 | 33 ± 14 |
| 4m | 2-Naphthyl- | 131 | stable | 76 ± 21 | 68 ± 6 |
| 4n | 2-Furanoyl | n.d. | n.d. | - | - |
| 6 | α -Fucosyl benzamide | stable | stable | 24 ± 8 | 78 ± 20 |
| 8a | Fucosyl benzene-sulfonamide | stable | stable | 33 ± 7 | 50 ± 7 |
| 8b | Fucosyl thiophene-2-sulfonamide | 123 | 112 | 100 ± 0 | 15 ± 9 |

n.d. = not detected; stable \geq 240 min.

Table 4: Metabolic stability of α/β -fucosyl amides and sulfonamides in mouse or human liver microsomes.

| No. | Structure | Mouse | | Human | |
|-----------|---|--------------------|---|--------------------|---|
| | | $t_{1/2}$ [min] | Cl_{int} [$\mu\text{L min}^{-1}$ mg^{-1} [protein]] | $t_{1/2}$ [min] | Cl_{int} [$\mu\text{L min}^{-1}$ mg^{-1} [protein]] |
| |  | | | | |
| 4a | Ph- | 27.7 | 179.3 | 23.7 | 58.4 |
| 4b | 2-Thiophenyl- | > 60 | < 23 | 34.8 | 39.8 |
| 4c | <i>p</i> CH ₃ -C ₆ H ₄ - | 22.4 | 61.8 | 11.5 | 120.4 |
| 4d | <i>p</i> MeO-C ₆ H ₄ - | > 60 | < 23 | 161.6 | 8.6 |
| 4e | <i>p</i> NO ₂ -C ₆ H ₄ - | 50.2 | 27.5 | 32.6 | 42.5 |
| 4f | <i>p</i> Cl-C ₆ H ₄ - | 69.4 | 20.0 | 119.1 | 11.6 |
| 4g | <i>p</i> CF ₃ -C ₆ H ₄ - | 161.8 | 8.6 | 229.7 | 6.0 |
| 4h | <i>m</i> CH ₃ -C ₆ H ₄ - | 47.0 | 29.5 | 146.4 | 9.5 |
| 4i | <i>m</i> Ph-C ₆ H ₄ - | 75.3 | 18.4 | > 60 | < 23 |
| 4j | CH ₃ - | > 60 | < 23 | 86.4 | 16.0 |
| 4k | (CH ₃) ₂ CH- | > 60 | < 23 | 25.2 | 55.0 |
| 4l | (<i>E</i>)-PhCH=CH- | > 60 | < 23 | 247.2 | 5.6 |
| 4m | 2-Naphthyl- | 27.6 | 50.2 | 65.7 | 21.1 |
| 4n | 2-Furanyl- | 104.4 | 13.3 | 59.6 | 23.2 |
| 6 | α -Fucosyl benzamide | 89.9 | 15.4 | 83.7 | 16.5 |
| 8a | α/β -Fucosyl benzenesulfonamide | > 60 | < 23 | > 60 | < 23 |
| 8b | α/β -Fucosyl thiophene-2- sulfonamide | 56.1 | 24.7 | 43.9 | 31.5 |

Then, the compounds were tested for their stability in presence of mouse or human liver microsomes (Table 4). Most compounds exhibited a rather low clearance, both in the presence of mouse microsomes (11/17 compounds $Cl_{int}(m) < 23 \mu\text{L min}^{-1} \text{mg}^{-1}$ [protein]) and human liver microsomes (10/17 compounds $Cl_{int}(h) < 23 \mu\text{L min}^{-1} \text{mg}^{-1}$ [protein]). *meta*-Methylbenzamide **4h** gave a moderate clearance with mouse microsomes ($Cl_{int}(m, \mathbf{4h}) = 30 \mu\text{L min}^{-1} \text{mg}^{-1}$ [protein]), and low clearance with human liver microsomes ($Cl_{int}(h, \mathbf{4h}) = 10 \mu\text{L min}^{-1} \text{mg}^{-1}$ [protein]). In contrast, its *para*-methyl isomer **4c** showed high clearance with microsomes of both species ($Cl_{int}(m, \mathbf{4c}) = 61 \mu\text{L min}^{-1} \text{mg}^{-1}$ [protein], $Cl_{int}(h, \mathbf{4c}) = 120 \mu\text{L min}^{-1} \text{mg}^{-1}$ [protein]). Interestingly, the two most potent inhibitors **4a** and **4i** behaved completely differently. While benzamide **4a** resulted in the highest intrinsic clearance with mouse and the second highest clearance with human liver microsomes ($Cl_{int}(\text{mouse}, \mathbf{4a}) = 179 \mu\text{L min}^{-1} \text{mg}^{-1}$ [protein];

CL_{int} (human, **4a**) = 58.4 $\mu\text{L min}^{-1} \text{mg}^{-1}$ [protein], biphenyl **4i** showed low clearance CL_{int} (**4i** < 23 $\mu\text{L min}^{-1} \text{mg}^{-1}$ [protein]) in presence of microsomes from both species. In general, several tested compounds had a good metabolic stability in the presence of mouse or human microsomes *in vitro* with $t_{1/2} > 60$ min, except for the *para/meta*-methyl benzamides **4c** and **4h**, unsubstituted benzamide **4a**, and naphthyl **4m**. Nitrophenyl **4e**, thiophenyl **4b** and furanyl **4n** were moderately stable with half-lives between $t_{1/2} = 47\text{--}56$ min in mouse and $t_{1/2} = 25\text{--}60$ min in human liver microsomes.

Furthermore, cytotoxicity of α -/ β -fucosyl amides and sulfonamides was assessed *in vitro* using three different cell lines, i.e., epithelial lung cell line (A549), Chinese hamster ovary cells (CHO) and epithelial liver cell line (HepG2) (**Figure 4**). All tested LecB ligands displayed no toxicity against A549 cells at 10 nM and 1000 nM. One exception was obtained for the amide derivative **4j** with slightly reduced viability at 1 μM . Testing against Chinese hamster ovary cells (CHO) also revealed no toxicity for most of the tested compounds. However, a noticeable dose-dependent toxicity was observed in the case of the two amide derivatives **4d** and **4j**. Finally, the testing against HepG2 liver epithelial cells resulted in heterogeneous cytotoxicity across our compounds. Eleven out of 15 fucosyl amides showed detectable cytotoxicity with in part strong reduction of cellular viability. Four exceptions devoid of detectable cytotoxicity against HepG2 cells were *para*-nitrophenyl amide **4e**, *meta*-methylphenyl amide **4h**, 2-furanoyl amide **4n** as well as biphenyl amide **4j**, a compound that was however somewhat toxic against the other two cell lines, A549 and CHO cells. No cytotoxicity against HepG2 cells was detected for sulfonamide **8a** while sulfonamide **8b** displayed significant cytotoxicity at 1000 nM.

In summary, all fucosyl amides were sufficiently stable in human plasma and most withstood degradation by human liver microsomes. Their intrinsic clearance was generally good except for benzamide **4a**, *para*-methylbenzamide **4c**, and for 2-naphthyl **4m**. With regard to cytotoxicity, a large variation was observed between the three tested cell lines and the 15 tested amides. Numerous compounds showed significant cytotoxicity especially against HepG2 cells, however some compounds did not show acute cytotoxicity in all three cell lines.

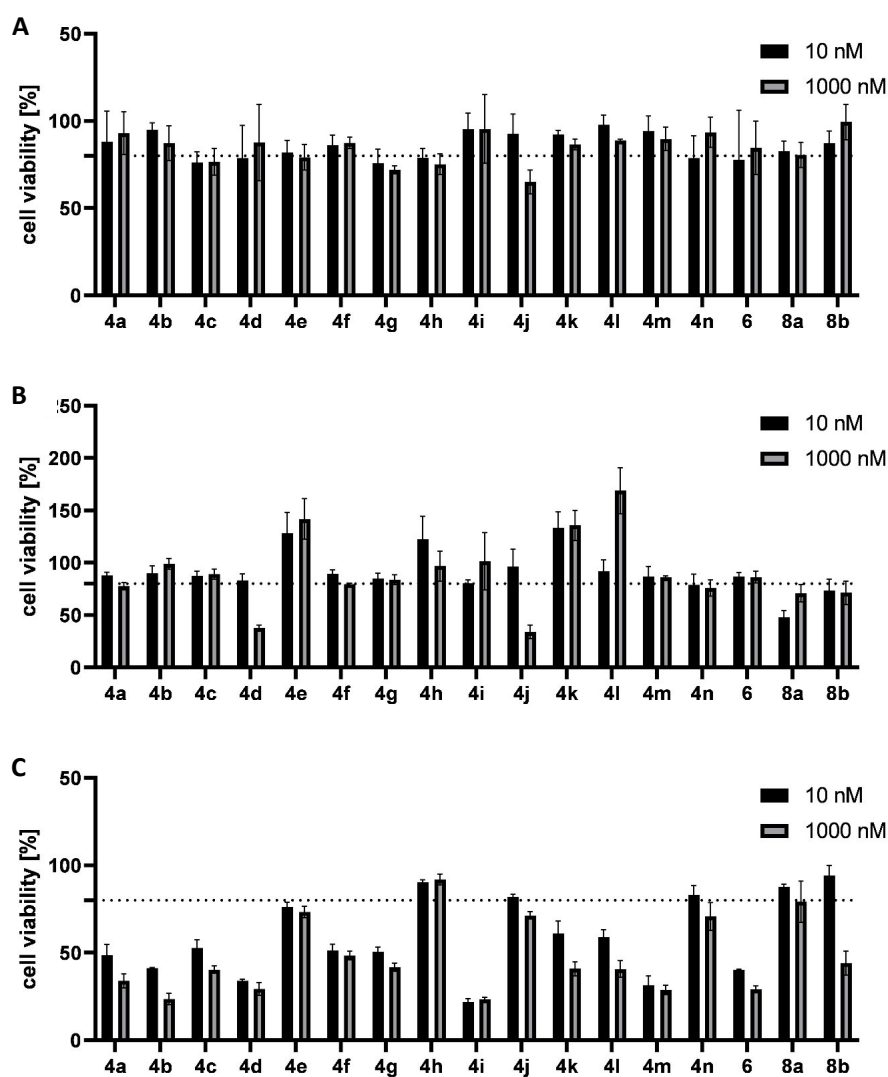


Figure 4: Cytotoxicity of α - β -fucosyl amides and sulfonamides against the lung epithelial cells A549 (**A**), Chinese hamster ovary cells (CHO) (**B**) and liver epithelial cells (HepG2) (**C**) at 10 nM and 1000 nM concentration of LecB ligands. Cells treated with vehicle only (DMSO diluted in PBS, final DMSO concentration in the cell assay: 0.1 %) served as a negative control indicated as the dashed line. Pure medium (DMEM + 10 % FCS) and completely damaged cells served as positive controls. The error bars show the standard deviation of minimum three independent experiments.

Conclusion

In our search for novel LecB inhibitors, we have designed and synthesized fucosylmethyl thioureas as well as shortened molecules, fucosyl amides and sulfonamides, lacking the methylene group in order to analyze the altered linker position on LecB binding. Surprisingly, the fucosylmethyl thioureas only showed moderate binding in the micromolar range which was also observed for the *N*-linked fucosyl sulfonamides. On the other hand, our β -fucosyl amides devoid of the methylene bridge constitute the first monovalent two-digit nanomolar LecB inhibitors with IC_{50} of 88 nM for benzamide **4a** and 85 nM for biphenyl derivative **4i**. Noteworthy,

α -fucosyl amides had been studied before with LecB and these molecules showed moderate micromolar affinities⁴⁵, which was confirmed by our control molecule α -benzamide **6**.

In the co-crystal structure of β -linked **4i** in complex with LecB, we demonstrated that the amide function is crucial for binding by forming a hydrogen bond with Ser22 which is located between the carbohydrate binding site and the additional subpocket, that is occupied by the proximal aromatic ring which hydrophobically interacts with Gly24 and Val69. These interactions are absent in the crystal structure of the α -anomer **6** in complex with LecB. Both crystal structures provide a basis for the interpretation of the microcalorimetric titration data for LecB with **4a** or **4i**. Compounds have also been analyzed for *in vitro* early ADME/Tox. In general, satisfying properties could be identified in all assays, except for significant cytotoxicity against one out of the three tested cell lines. Despite the fact that numerous compounds proved toxic, the presence of several derivatives without detectable cytotoxicity clearly underlines their potential for future optimization.

During the writing of this manuscript, a set of β -fucosyl amides has been reported as weak inhibitors of the N-terminal domain of BC2L-C, a lectin from *Burkholderia cenocepacia*^{46,47}, that also binds fucose but displays different sequence, structure and binding site architecture compared to LecB. Despite this low affinity, further optimization could open a possibility for a molecule that potently inhibits both lectins, which could be of interest since *P. aeruginosa* and *B. cenocepacia* often co-infect cystic fibrosis patients. Thus, these β -fucosyl amides constitute a promising new class of LecB inhibitors for future use as pathoblockers against infections with *P. aeruginosa* and beyond.

Material and Methods

General experimental details and syntheses are described in the supporting information.

Docking

The crystal structure coordinates of LecB in complex with fucose (pdb: 1OXC) was adjusted for docking in MOE (Molecular Operating Environment, Chemical Computing Group, Canada version: 2014.0901) by removing all ligands and water molecules and keeping one monomer. The coordinates of the carbohydrate binding site were determined in AutoDockTools⁴⁸ and added into the docking-file. Four amino acid Asn21, Glu95, Asp101 and Asn103 were kept flexible during the docking-run. In parallel, ligands for docking were drawn in ChemDraw, exported as SMILES code and translated into a pdb-file using the online SMILES Translator.⁴⁹ The ligand pdb-files were processed in MOE, bonds were set to the lowest energy level, and

exported as a mol2-file and added to the docking file. The docking was performed with Plants1.1⁵⁰ using a binding site radius of 13 Å. For validation of the protocol, docking was performed first with α -L-fucose and the resulting pose was then superimposed with its co-crystal structure in the Molecular Operating Environment (MOE), which confirmed the same interactions. Afterwards, the two compounds **4a** and **11c**, were docked. The results were visualized and analyzed in MOE.

Recombinant Expression and Purification of LecB

LecB from *P. aeruginosa* PAO1 was expressed and purified from *Escherichia coli* BL21 (DE3) and the plasmid pET25pa2I⁵¹ as described before.³⁷

Competitive Binding Assay

The competitive binding assay based on fluorescence polarization was performed with small modifications in analogy to the one described before.¹³ To a 10 μ L solution of LecB_{PAO1} (150 nM) and the fluorescent reporter ligand (*N*-(fluorescein-5-yl)-*N'*-(α -L-fucosyl ethylene)-thiocarbamide, 20 nM) in TBS/Ca²⁺-buffer containing 0.02% DMSO (20 mM Tris*HCl, 137 mM NaCl, 2.6 mM KCl, 1 mM CaCl₂, pH = 7.4) in a black 384-well plate (Greiner Bio-One, Germany, cat. no. 781900), a 10 μ L serial dilution of the inhibitor in the same buffer (10–0.005 μ M, dilution factor 2) was added (technical triplicates). The plate was sealed (EASYseal, Greiner Bio-One, cat. no. 676001), centrifuged (1500 x g, r.t., 1 min) and incubated in a dark chamber under shaking conditions for 24 h. Afterwards, the seal was removed and fluorescence was measured on a PHERAstar FS (BMG Labtech, Germany, filter ex.: 485 nm em.: 535 nm). After blank value (TBS/Ca²⁺-buffer with LecB) subtraction from the measured fluorescence intensities, polarization was calculated and the data were analyzed using the four-parameter variable slope model in MARS software (BMG Labtech). Then, top and bottom plateaus were redefined using the full inhibition value in presence of the positive control L-fucose and full binding value for LecB and reporter ligand in the absence of inhibitor as a negative control. The experiments were performed in three independent experiments, the data were averaged and visualized using GraphPad PRISM (version 5). Fucosylmethyl thioureas were tested at a final LecB concentration of 150 nM, a dilution series 100–0.78 μ M and 0.1% DMSO in the TBS/Ca²⁺-buffer.

Isothermal Titration Calorimetry

Compounds **4a**, **6** and LecB_{PAO1} were separately dissolved in the same TBS/Ca²⁺-buffer and the concentration for LecB was determined by UV absorbance (ϵ = 6990 M⁻¹ cm⁻¹⁵²). Experiments were performed on a MicroCal iTC₂₀₀ (Malvern Panalytical, United Kingdom)

instrument by titrating the ligand (500–1500 μM) into LecB solution (100 μM) with stirring (700 rpm) at 25 °C. The reference power was set to 5 $\mu\text{cal s}^{-1}$, the filter period to 5 s, and 19–39 injections (0.5–2 μL per injection) with an injection duration of 1 s and a spacing of 240 s between each injection were performed per experiment. In case of titrations with lower LecB concentrations (500 μM), the syringe was refilled after the first run ended, and the experiments were continued with the same sample cell contents to reach saturation. The resulting data files were merged with the MicroCal Concat ITC software. The first injection of every titration was discarded and the data were analyzed with the MicroCal Origin software using the one-site binding model. ITC data are depicted in **Figure 2** and **Table SI 1**.

X-ray Crystallography of LecB_{PAO1} in complex with 6 or 4i:

LecB_{PAO1} at 10.8 mg mL⁻¹ in water with 1 mM CaCl₂ (**4a** and **4i**) or at 9.3 mg mL⁻¹ in 20 mM HEPES pH 7.5, 100 mM NaCl and 100 μM CaCl₂ (**6**) was incubated in a 19:1 ratio with 2.5 mM of compound for 30 min to 1 h prior to crystallization. Stock solution at 50 mM of compound were made in water for **4a** and in 100% DMSO for **4i** and **6**. Hanging drop vapor diffusion method using 1 μL of protein-ligand mixture with 1 μL of reservoir solution at 19 °C in a 24-well plate yielded crystals after 1–3 days. The crystals for the LecB_{PAO1}-**4a** or LecB_{PAO1}-**4i** complexes were obtained with 30 and 28% PEG 8K, 200 mM (NH₄)₂SO₄ and 100 mM Tris pH = 8.5, respectively and those for LecB_{PAO1}-**6** with 24% Peg8K, 1 M LiCl and 100 mM sodium acetate pH 4.4. All solutions were cryoprotected and the crystal was directly mounted in a cryoloop and flash-frozen in liquid nitrogen. Diffraction data were collected at 100 K at Synchrotron SOLEIL (Paris, France) on beamline Proxima 1 using an EIGER X 16M area detector for LecB_{PAO1}-**4a** and LecB_{PAO1}-**4i** or Proxima 2 using a EIGER X 9M area detector for LecB_{PAO1}-**6**. The data were processed using XDS and XDSme.^{53,54} All further computing was performed using the CCP4 suite.⁵⁵ Five percent of the observations were set aside for cross validation analysis and hydrogen atoms were added in their riding positions, and used for geometry and structure-factor calculations. The structure was solved by molecular replacement using PHASER.⁵⁶ For complexes with **4i** and **6**, the coordinates of the 5A3O tetramer were used as a search model to search for one tetramer in the asymmetric unit. The structures were refined with restrained maximum likelihood refinement using REFMAC 5.8⁵⁷, iterated with manual rebuilding in Coot.⁵⁸ Ligand libraries were created using JLigand. The ligands were introduced after inspection of the 2Fo – DFc weighted maps. Water molecules, introduced automatically using Coot, were inspected manually. The stereochemical quality of the models was assessed with the PDB Validation Server. The structure of LecB in complex with **4a** was solved by molecular replacement at 2.5 Å using Phaser and a search for one tetramer and 2 dimers from model 1GZT. The low resolution did not give suitable electron density and we

decided not to refine it. Data quality and refinement statistics are summarized in Supporting Information, **Table SI 4**. All structural figures were created using PyMOL.

Plasma Stability Assay

Each compound, dissolved in DMSO (10 mM), was added to mouse plasma (pH = 7.4, 37 °C) or to human plasma (pH = 7.4, 37 °C) to yield a final concentration of 1 µM. In addition, procaine and procainamide (dissolved in DMSO) were added to mouse plasma or to human plasma (pH = 7.4, 37 °C) to yield a final concentration of 1 µM. Procaine served as a positive control as it is unstable in mouse plasma. Procainamide served as a negative control as it is stable in mouse plasma. The samples were incubated for 0, 15, 30, 60, 90, 120, and 240 min at 37 °C. At each time point, 10 µL of the respective sample was extracted with 90 µL acetonitrile and 12.5 ng/mL of caffeine as an internal standard for 5 min at 2000 rpm on a MixMate vortex mixer (Eppendorf). Acetonitrile and caffeine were dispensed using a Mantis Formulatrix. Then samples were centrifuged for 20 min at 2270 x g at 4 °C and the supernatants were transferred to 96-well Greiner V-bottom plates. Peak areas of each compound and of the internal standard were analyzed using the MultiQuant 3.0 software (AB Sciex). Peak areas of the respective compound were normalized to the internal standard peak area and to the respective peak areas at time point 0 min with equation (1):

$$Norm_{peak\ area} = \frac{C * D^{-1}}{A * B^{-1}} \quad (1)$$

A: peak area of the compound at the time point 0 min, B: peak area of the internal standard at time point 0 min, C: peak area of the compound at the respective time point, D: peak area of the internal standard at the respective time point.

In vitro Metabolic Stability Assay

Liver microsomes (mouse and human, Thermo Fisher) were thawed slowly on ice. 5 mg mL⁻¹ of microsomes, 2 µL of a 100 µM solution of every compound and 183 µL of 100 mM phosphate buffer were incubated 5 min at 37 °C in a water bath. Reactions were initiated using 10 µL of 20 mM NADPH (CarlRoth, Germany). Samples were incubated in three replicates at 37 °C under gentle agitation at 150 rpm. At 0, 5, 15, 30, and 60 min, reactions were terminated by the addition of 180 µL acetonitrile. Samples were vortexed for 5 min and then centrifuged at 2270 x g for 20 min at 4 °C. The supernatants were transferred to 96-well Greiner V-bottom plates, sealed with WebSeal non-sterile mats (Thermo Fisher) and analyzed according to the section HPLC-MS analysis. Peak areas of the respective time point of the compounds were normalized to the peak area at time point 0 min. Then half-life was calculated using linear regression. Cl_{int} [µL/min/mg protein] was calculated using the following equation (2):

$$CL_{int} [\mu\text{L min}^{-1} \text{mg}_{(\text{protein})}^{-1}] = \frac{0.693}{0.005 * t_{1/2}} \quad (2)$$

Plasma Protein Binding

Plasma protein binding was assessed using the rapid equilibrium device (RED) system from ThermoFisher. Compounds were dissolved in DMSO to a concentration of 10 mM. Naproxene served as control as it shows high plasma protein binding. Compounds were diluted in murine plasma (from CD-1 mice, pooled, Biomol GmbH) or in human plasma (human donors, both genders, pooled, antibodies-online GmbH) to a final concentration of 1 μM . Dialysis buffer and plasma samples were added to the respective chambers according to the manufacturer's protocol. The RED plate was sealed with a tape and incubated at 37 °C for 2 hours at 800 rpm on an Eppendorf MixMate vortex-mixer. Then samples (dialysis and plasma samples) were withdrawn from the respective chambers. To 25 μL of each dialysis sample, 25 μL of plasma and to 25 μL of plasma sample, 25 μL of dialysis buffer was added. Then, 150 μL ice-cold extraction solvent (ACN/H₂O (90:10) containing 12.5 ng mL⁻¹ caffeine as internal standard) was added. Samples were incubated for 30 min on ice. Then, samples were centrifuged at 4 °C at 2270 x g for 10 min. Supernatants were transferred to Greiner V-bottom 96-well plates and sealed with a tape. The percentage of bound compound was calculated with the equations (3) and (4):

$$\%_{free} = \frac{C_{buffer\ chamber}}{C_{plasma\ chamber}} * 100 \quad (3)$$

$$\%_{bound} = 100\% - \%_{free} \quad (4)$$

HPLC-MS Analysis

Samples were analyzed using an Agilent 1290 Infinity II HPLC system coupled to an AB Sciex QTrap 6500plus mass spectrometer. LC conditions were as follows: column: Agilent Zorbax Eclipse Plus C18, 50x2.1 mm, 1.8 μm ; temperature: 30 °C; injection volume: 5 μL per sample; flow rate: 700 $\mu\text{L min}^{-1}$. Samples were run under acidic and buffered conditions. Solvents for acidic conditions: A1: water + 0.1% formic acid; solvent B1: 95% acetonitrile/5% H₂O + 0.1% formic acid; solvents for buffered conditions: A2: 95% H₂O + 5% acetonitrile + 5 mM ammonium acetate + 40 $\mu\text{L L}^{-1}$ acetic acid; B2: 95% acetonitrile + 5 % H₂O + 5 mM ammonium acetate + 40 $\mu\text{L L}^{-1}$ acetic acid. The same gradient was applied for acidic and buffered conditions: 99% A at 0 min, 99% A until 1 min, 99–0% A from 1.0 min to 4.0 min, 0% A until 5.0 min. Mass transitions for controls and compounds are depicted in **Table SI 4**.

Cytotoxicity

The epithelial liver cell line HepG2 (ATCC HB-8065TM) and the epithelial lung cell line A549 (ATCC CCL-185) were cultivated in Dulbecco's modified Eagle's medium (DMEM) with 10% heat-inactivated fetal calf serum (FCS) at 37°C and 5% CO₂. CHO cells (ATCC CCL-61) were cultivated in Gibco Ham's F-12K medium supplemented with 10% FCS. Cells were seeded into a 96-well plate (Nunc, Roskilde, Denmark) and grown to 75% confluency. The following compounds were tested in the cell assay: **4a-4n**, **6**, **8a** and **8b**. Every compound was dissolved in DMSO and diluted in PBS (final DMSO concentration in the cell assay: 0.1 %). Cells were incubated for 24 h at 37°C and 5% CO₂ with the respective compound at two different concentrations (10 nM and 1 μM) allowing for a rapid screen. Cells treated with vehicle only (DMSO diluted in PBS, final DMSO concentration in the cell assay: 0.1 %) served as a negative control. Furthermore, pure medium (DMEM + 10 % FCS) and completely damaged cells served as positive controls. To damage cells, cells were treated with 0.5% Triton X-100 1 h prior to addition of MTT (Sigma). After 24 h cells were washed twice with DMEM + 10% FCS (A549 and HepG2 cells) or Ham's F-12K + 10% FCS (CHO-cells). MTT diluted in PBS (stock solution 5 mg/mL) was added to the wells at a final concentration of 1 mg/mL. The cells were incubated for 3 h at 37°C and 5% CO₂. Medium was removed and 0.04 M HCl in 2-propanol was added. The cells were incubated at room temperature for 15 min. Then the supernatant was transferred to a 96-well plate. UV absorbance of the samples was measured at 560 nm and at 670 nm as a reference wavelength on a Tecan Sunrise ELISA reader using Magellan software. Data was normalized using the following formula: $(A-B)/(C-B)$ with 'A' as the respective data point, 'B' as the value of the Triton X-100-treated control and 'C' as the vehicle control. The experiment was repeated at least three times. The error bars indicate the standard deviation.

Supporting Information

The supporting information contain synthesis procedures of LecB inhibitors, transcripts of ¹H- and ¹³C-NMR spectra of new compounds, purity of key compounds by LCMS, protein-ligand interaction maps of the docked compounds, β-fucosyl benzamide **4a** and β-fucosylmethyl thiourea **11c**, ITC data of all replicates for titrations of LecB with β-/α-fucosyl benzamides **4a** and **6**, X-ray data collection and refinement statistics of LecB complexed structures and a zoom in the electron density and interactions of the ligand with each LecB protomers, and m/z search window for plasma stability and mass transitions of the tested compounds from the ADME studies.

Orcid

Patrycja Mała: 0000-0002-1259-6484

Eike Siebs: 0000-0002-7349-9872

Joscha Meiers: 0000-0003-0869-0088

Katharina Rox: 0000-0002-8020-1384

Annabelle Varrot: 0000-0001-6667-8162

Anne Imberty: 0000-0001-6825-9527

Alexander Titz: 0000-0001-7408-5084

Notes

The authors declare no competing financial interest.

Acknowledgements

A.T. and A.I. acknowledge by financial support of the French-German ANR/DFG project (ANR-AAPG-2017) funded by the Agence Nationale de la Recherche (grant no. ANR-17-CE11-0048) and Deutsche Forschungsgemeinschaft (grant no. Ti756/5-1). A.I and A.V. acknowledge support from ANR project Glyco@Alps (ANR-15-IDEX-02), Labex ARCANE, and CBH-EUR-GS (ANR-17-EURE-0003). The authors also thank DAAD for a scholarship to P.M., acknowledge grant no. POWR.03.02.00-00-I026/16 co-financed by the European Union through the European Social Fund under the Operational Program Knowledge Education Development, for her support, the Ambassade de France en Allemagne for a PROCOPE-Mobility scholarship to J.M., and the European Research Council for an ERC Starting Grant (Sweetbullets, grant no 716311) to A.T. KR receives support from the German Centre for Infection Research (DZIF, TTU 09.719) for operating the PK/PD unit. We acknowledge the synchrotron SOLEIL (Saint Aubin, France) for access to beamlines Proxima 1 and 2 (Proposal Number 20191314) and for the technical support of Pierre Montaville and Martin Savko. We also acknowledge Yasmina Grimoire, Emilie Gillon (both CERMAV), Dirk Hauck (HIPS), Janine Schreiber and Kimberley Vivien Sander (both HZI) for excellent technical support.

References

- (1) Miethke, M.; Pieroni, M.; Weber, T.; Brönstrup, M.; Hammann, P.; Halby, L.; Arimondo, P. B.; Glaser, P.; Aigle, B.; Bode, H. B.; Moreira, R.; Li, Y.; Luzhetskyy, A.; Medema, M. H.; Pernodet, J. L.; Stadler, M.; Tormo, J. R.; Genilloud, O.; Truman, A. W.; Weissman, K. J.; Takano, E.; Sabatini, S.; Stegmann, E.; Brötz-Oesterhelt, H.; Wohlleben, W.; Seemann, M.; Empting, M.; Hirsch, A. K. H.; Loretz, B.; Lehr, C. M.; Titz, A.; Herrmann, J.; Jaeger, T.; Alt, S.; Hesterkamp, T.; Winterhalter, M.; Schiefer, A.; Pfarr, K.; Hoerauf, A.; Graz, H.; Graz, M.; Lindvall, M.; Ramurthy, S.; Karlén, A.; van Dongen, M.; Petkovic, H.; Keller, A.; Peyrane, F.; Donadio, S.; Fraisse, L.; Piddock, L. J. V.; Gilbert, I. H.; Moser, H. E.; Müller, R. Towards the Sustainable Discovery and Development of New Antibiotics. *Nat. Rev. Chem.* **2021**, *5* (10), 726–749. <https://doi.org/10.1038/s41570-021-00313-1>.
- (2) World Health Organization. WHO publishes list of bacteria for which new antibiotics are urgently needed www.who.int/news/item/27-02-2017-who-publishes-list-of-bacteria-for-which-new-antibiotics-are-urgently-needed.
- (3) Wagner, S.; Sommer, R.; Hinsberger, S.; Lu, C.; Hartmann, R. W.; Empting, M.; Titz, A. Novel Strategies for the Treatment of Pseudomonas Aeruginosa Infections. *J. Med. Chem* **2016**, *59*, 5929–5969. <https://doi.org/10.1021/acs.jmedchem.5b01698>.
- (4) Spoering, A. L.; Lewis, K. Biofilms and Planktonic Cells of Pseudomonas Aeruginosa Have Similar Resistance to Killing by Antimicrobials. *J. Bacteriol.* **2001**, *183* (23), 6746–6751. <https://doi.org/10.1128/JB.183.23.6746-6751.2001>.
- (5) Rasamiravaka, T.; Labtani, Q.; Duez, P.; Jaziri, M. El. The Formation of Biofilms by Pseudomonas Aeruginosa: A Review of the Natural and Synthetic Compounds Interfering with Control Mechanisms. *Biomed Res. Int.* **2015**, *2015*, 1–17.
- (6) Carmeli, Y.; Troillet, N.; Eliopoulos, G. M.; Samore, M. H. Emergence of Antibiotic-Resistant Pseudomonas Aeruginosa: Comparison of Risks Associated with Different Antipseudomonal Agents. *Antimicrob. Agents Chemother.* **1999**, *43* (6), 1379–1382. <https://doi.org/10.1128/aac.43.6.1379>.
- (7) Calvert, M. B.; Jumde, V. R.; Titz, A. Pathoblockers or Antivirulence Drugs as a New Option for the Treatment of Bacterial Infections. *Beilstein J. Org. Chem.* **2018**, *14* (1), 2607–2617. <https://doi.org/10.3762/BJOC.14.239>.
- (8) Diggle, S. P.; Stacey, R. E.; Dodd, C.; Cámara, M.; Williams, P.; Winzer, K. The Galactophilic Lectin, LecA, Contributes to Biofilm Development in Pseudomonas Aeruginosa. *Environmental Microbiology.* 2006, pp 1095–1104.

<https://doi.org/10.1111/j.1462-2920.2006.001001.x>.

- (9) Tielker, D.; Hacker, S.; Loris, R.; Strathmann, M.; Wingender, J.; Wilhelm, S.; Rosenau, F.; Jaeger, K. E. Pseudomonas Aeruginosa Lectin LecB Is Located in the Outer Membrane and Is Involved in Biofilm Formation. *Microbiology* **2005**, *151* (5), 1313–1323. <https://doi.org/10.1099/mic.0.27701-0>.
- (10) Imberty, A.; Wimmerová, M.; Mitchell, E. P.; Gilboa-Garber, N. Structures of the Lectins from Pseudomonas Aeruginosa: Insights into the Molecular Basis for Host Glycan Recognition. *Microbes Infect.* **2004**, *6* (2), 221–228. <https://doi.org/10.1016/J.MICINF.2003.10.016>.
- (11) Passos Da Silva, D.; Matwichuk, M. L.; Townsend, D. O.; Reichhardt, C.; Lamba, D.; Wozniak, D. J.; Parsek, M. R. The Pseudomonas Aeruginosa Lectin LecB Binds to the Exopolysaccharide Psl and Stabilizes the Biofilm Matrix. *Nat. Commun.* **2019**, *10*, 2183. <https://doi.org/10.1038/s41467-019-10201-4>.
- (12) Chemani, C.; Imberty, A.; De Bentzmann, S.; Pierre, M.; Wimmerová, M.; Guery, B. P.; Faure, K. Role of LecA and LecB Lectins in Pseudomonas Aeruginosa-Induced Lung Injury and Effect of Carbohydrate Ligands. *Infect. Immun.* **2009**, *77* (5), 2065–2075. <https://doi.org/10.1128/IAI.01204-08>.
- (13) Sommer, R.; Wagner, S.; Varrot, A.; Nycholat, C. M.; Khaledi, A.; Häussler, S.; Paulson, J. C.; Imberty, A.; Titz, A. The Virulence Factor LecB Varies in Clinical Isolates: Consequences for Ligand Binding and Drug Discovery. *Chem. Sci.* **2016**, *7* (8), 4990–5001. <https://doi.org/10.1039/c6sc00696e>.
- (14) Boukerb, A. M.; Decor, A.; Ribun, S.; Tabaroni, R.; Rousset, A.; Commin, L.; Buff, S.; Doléans-Jordheim, A.; Vidal, S.; Varrot, A.; Imberty, A.; Cournoyer, B. Genomic Rearrangements and Functional Diversification of LecA and LecB Lectin-Coding Regions Impacting the Efficacy of Glycomimetics Directed against Pseudomonas Aeruginosa. *Front. Microbiol.* **2016**, *7* (May), 1–16. <https://doi.org/10.3389/fmicb.2016.00811>.
- (15) Eierhoff, T.; Bastian, B.; Thuenauer, R.; Madl, J.; Audfray, A.; Aigal, S.; Juillot, S.; Rydell, G. E.; Muller, S.; de Bentzmann, S.; Imberty, A.; Fleck, C.; Romer, W. A Lipid Zipper Triggers Bacterial Invasion. *Proc. Natl. Acad. Sci.* **2014**, *111* (35), 12895–12900. <https://doi.org/10.1073/pnas.1402637111>.
- (16) Zheng, S.; Eierhoff, T.; Aigal, S.; Brandel, A.; Thuenauer, R.; de Bentzmann, S.; Imberty, A.; Römer, W. The Pseudomonas Aeruginosa Lectin LecA Triggers Host Cell Signalling by Glycosphingolipid-Dependent Phosphorylation of the Adaptor Protein CrkII. *Biochim.*

Biophys. Acta - Mol. Cell Res. **2017**, *1864* (7), 1236–1245.
<https://doi.org/10.1016/J.BBAMCR.2017.04.005>.

- (17) Thuenauer, R.; Landi, A.; Trefzer, A.; Altmann, S.; Wehrum, S.; Eierhoff, T.; Diedrich, B.; Dengjel, J.; Nyström, A.; Imberty, A.; Römer, W. The *Pseudomonas Aeruginosa* Lectin LecB Causes Integrin Internalization and Inhibits Epithelial Wound Healing. *Am. Soc. Microbiol.* **2020**, *11* (2), e03260-19.
- (18) Hauber, H. P.; Schulz, M.; Pforte, A.; Mack, D.; Zabel, P.; Schumacher, U. Inhalation with Fucose and Galactose for Treatment of *Pseudomonas Aeruginosa* in Cystic Fibrosis Patients. *Int. J. Med. Sci.* **2008**, *5* (6), 371–376. <https://doi.org/10.7150/ijms.5.371>.
- (19) Bucior, I.; Abbott, J.; Song, Y.; Matthay, M. A.; Engel, J. N. Sugar Administration Is an Effective Adjunctive Therapy in the Treatment of *Pseudomonas Aeruginosa* Pneumonia. *Am. J. Physiol. - Lung Cell. Mol. Physiol.* **2013**, *305* (5), 1–22. <https://doi.org/10.1152/ajplung.00387.2012>.
- (20) Cecioni, S.; Imberty, A.; Vidal, S. Glycomimetics versus Multivalent Glycoconjugates for the Design of High Affinity Lectin Ligands. *Chem. Rev.* **2015**, *115* (1), 525–561. <https://doi.org/10.1021/cr500303t>.
- (21) Meiers, J.; Siebs, E.; Zahorska, E.; Titz, A. Lectin Antagonists in Infection, Immunity, and Inflammation. *Curr. Opin. Chem. Biol.* **2019**, *53*, 51–67. <https://doi.org/10.1016/j.cbpa.2019.07.005>.
- (22) Cioci, G.; Mitchell, E. P.; Gautier, C.; Wimmerová, M.; Sudakevitz, D.; Pérez, S.; Gilboa-Garber, N.; Imberty, A. Structural Basis of Calcium and Galactose Recognition by the Lectin PA-IL of *Pseudomonas Aeruginosa*. *FEBS Lett.* **2003**, *555* (2), 297–301. [https://doi.org/10.1016/S0014-5793\(03\)01249-3](https://doi.org/10.1016/S0014-5793(03)01249-3).
- (23) Joachim, I.; Rikker, S.; Hauck, D.; Ponader, D.; Boden, S.; Sommer, R.; Hartmann, L.; Titz, A. Development and Optimization of a Competitive Binding Assay for the Galactophilic Low Affinity Lectin LecA from *Pseudomonas Aeruginosa*. *Org. Biomol. Chem.* **2016**, *14* (33), 7933–7948. <https://doi.org/10.1039/C6OB01313A>.
- (24) Rodrigue, J.; Ganne, G.; Blanchard, B.; Saucier, C.; Giguère, D.; Shiao, T. C.; Varrot, A.; Imberty, A.; Roy, R. Aromatic Thioglycoside Inhibitors against the Virulence Factor LecA from *Pseudomonas Aeruginosa*. *Org. Biomol. Chem.* **2013**, *11* (40), 6906–6918. <https://doi.org/10.1039/c3ob41422a>.
- (25) Kadam, R. U.; Garg, D.; Schwartz, J.; Visini, R.; Sattler, M.; Stocker, A.; Darbre, T.;

Reymond, J.-L. CH- π "T-Shape" Interaction with Histidine Explains Binding of Aromatic Galactosides to *Pseudomonas Aeruginosa* Lectin LecA. *ACS Chem. Biol.* **2013**, *8* (9), 1925–1930. <https://doi.org/10.1021/cb400303w>.

- (26) Pertici, F.; de Mol, N. J.; Kemmink, J.; Pieters, R. J. Optimizing Divalent Inhibitors of *Pseudomonas Aeruginosa* Lectin LecA by Using A Rigid Spacer. *Chem. Eur. J.* **2013**, *19* (50), 16923–16927. <https://doi.org/10.1002/chem.201303463>.
- (27) Zahorska, E.; Kuhaudomlarp, S.; Minervini, S.; Yousaf, S.; Lepsik, M.; Kinsinger, T.; Hirsch, A. K. H.; Imberty, A.; Titz, A. A Rapid Synthesis of Low-Nanomolar Divalent LecA Inhibitors in Four Linear Steps from d-Galactose Pentaacetate. *Chem. Commun.* **2020**, *56* (62), 8822–8825. <https://doi.org/10.1039/d0cc03490h>.
- (28) Novoa, A.; Eierhoff, T.; Topin, J.; Varrot, A.; Barluenga, S.; Imberty, A.; Römer, W.; Winssinger, N. A LecA Ligand Identified from a Galactoside-Conjugate Array Inhibits Host Cell Invasion by *Pseudomonas Aeruginosa*. *Angew. Chem. Int. Ed. Int. Ed.* **2014**, *53* (34), 8885–8889. <https://doi.org/10.1002/anie.201402831>.
- (29) Wagner, S.; Hauck, D.; Hoffmann, M.; Sommer, R.; Joachim, I.; Müller, R.; Imberty, A.; Varrot, A.; Titz, A. Covalent Lectin Inhibition and Application in Bacterial Biofilm Imaging. *Angew. Chem. Int. Ed.* **2017**, *56* (52), 16559–16564. <https://doi.org/10.1002/anie.201709368>.
- (30) Siebs, E.; Shanina, E.; Kuhaudomlarp, S.; da Silva Figueiredo Celestino Gomes, P.; Fortin, C.; Seeberger, P. H.; Rognan, D.; Rademacher, C.; Imberty, A.; Titz, A. Targeting the Central Pocket of the *Pseudomonas Aeruginosa* Lectin LecA. *ChemBioChem* **2022**, *23* (3), e202100563. <https://doi.org/10.1002/cbic.202100563>.
- (31) Kuhaudomlarp, S.; Siebs, E.; Shanina, E.; Topin, J.; Joachim, I.; da Silva Figueiredo Celestino Gomes, P.; Varrot, A.; Rognan, D.; Rademacher, C.; Imberty, A.; Titz, A. Non-Carbohydrate Glycomimetics as Inhibitors of Calcium(II)-binding Lectins. *Angew. Chem. Int. Ed. Int. Ed.* **2021**, *60*, 8104–8114. <https://doi.org/10.1002/anie.202013217>.
- (32) Shanina, E.; Kuhaudomlarp, S.; Siebs, E.; Fuchsberger, F. F.; Denis, M.; Gomes, F. P. da S. C.; Clausen, M. H.; Seeberger, P. H.; Rognan, D.; Titz, A.; Imberty, A.; Rademacher, C. Targeting Undruggable Carbohydrate Recognition Sites through Focused Fragment Library Design. *Commun. Chem.* **2022**, *5*, 64. <https://doi.org/10.1038/s42004-022-00679-3>.
- (33) Mitchell, E.; Houles, C.; Sudakevitz, D.; Wimmerova, M.; Gautier, C.; Pérez, S.; Wu, A. M.; Gilboa-Garber, N.; Imberty, A. Structural Basis for Oligosaccharide-Mediated

Adhesion of *Pseudomonas Aeruginosa* in the Lungs of Cystic Fibrosis Patients. *Nat. Struct. Biol.* **2002**, *9* (12), 918–921. <https://doi.org/10.1038/nsb865>.

- (34) Sabin, C.; Mitchell, E. P.; Pokorná, M.; Gautier, C.; Utille, J. P.; Wimmerová, M.; Imberty, A. Binding of Different Monosaccharides by Lectin PA-IIL from *Pseudomonas Aeruginosa*: Thermodynamics Data Correlated with X-Ray Structures. *FEBS Lett.* **2006**, *580* (3), 982–987. <https://doi.org/10.1016/j.febslet.2006.01.030>.
- (35) Sommer, R.; Exner, T. E.; Titz, A. A Biophysical Study with Carbohydrate Derivatives Explains the Molecular Basis of Monosaccharide Selectivity of the *Pseudomonas Aeruginosa* Lectin LecB. *PLoS One* **2014**, *9* (11), 1–22. <https://doi.org/10.1371/journal.pone.0112822>.
- (36) Sommer, R.; Wagner, S.; Rox, K.; Varrot, A.; Hauck, D.; Wamhoff, E. C.; Schreiber, J.; Ryckmans, T.; Brunner, T.; Rademacher, C.; Hartmann, R. W.; Brönstrup, M.; Imberty, A.; Titz, A. Glycomimetic, Orally Bioavailable LecB Inhibitors Block Biofilm Formation of *Pseudomonas Aeruginosa*. *J. Am. Chem. Soc.* **2018**, *140* (7), 2537–2545. <https://doi.org/10.1021/jacs.7b11133>.
- (37) Hauck, D.; Joachim, I.; Frommeyer, B.; Varrot, A.; Philipp, B.; Möller, H. M.; Imberty, A.; Exner, T. E.; Titz, A. Discovery of Two Classes of Potent Glycomimetic Inhibitors of *Pseudomonas Aeruginosa* LecB with Distinct Binding Modes. *ACS Chem. Biol.* **2013**, *8* (8), 1775–1784. <https://doi.org/10.1021/cb400371r>.
- (38) Hofmann, A.; Sommer, R.; Hauck, D.; Stifel, J.; Göttker-Schnetmann, I.; Titz, A. Synthesis of Mannoheptose Derivatives and Their Evaluation as Inhibitors of the Lectin LecB from the Opportunistic Pathogen *Pseudomonas Aeruginosa*. *Carbohydr. Res.* **2015**, *412*, 34–42. <https://doi.org/10.1016/j.carres.2015.04.010>.
- (39) Sommer, R.; Hauck, D.; Varrot, A.; Wagner, S.; Audfray, A.; Prestel, A.; Möller, H. M.; Imberty, A.; Titz, A. Cinnamide Derivatives of D-Mannose as Inhibitors of the Bacterial Virulence Factor LecB from *Pseudomonas Aeruginosa*. *ChemistryOpen* **2015**, *4* (6), 756–767. <https://doi.org/10.1002/open.201500162>.
- (40) Sommer, R.; Rox, K.; Wagner, S.; Hauck, D.; Henrikus, S. S.; Newsad, S.; Arnold, T.; Ryckmans, T.; Brönstrup, M.; Imberty, A.; Varrot, A.; Hartmann, R. W.; Titz, A. Anti-Biofilm Agents against *Pseudomonas Aeruginosa*: A Structure-Activity Relationship Study of C-Glycosidic LecB Inhibitors. *J. Med. Chem.* **2019**, *62* (20), 9201–9216. <https://doi.org/10.1021/acs.jmedchem.9b01120>.
- (41) Allegretti, P. E.; Castro, E. A.; Furlong, J. J. P. Tautomeric Equilibrium of Amides and

Related Compounds: Theoretical and Spectral Evidences. *J. Mol. Struct. THEOCHEM* **2000**, 499 (1–3), 121–126. [https://doi.org/10.1016/S0166-1280\(99\)00294-8](https://doi.org/10.1016/S0166-1280(99)00294-8).

- (42) Damkaci, F.; DeShong, P. Stereoselective Synthesis of α - and β -Glycosylamide Derivatives from Glycopyranosyl Azides via Isoxazoline Intermediates. *J. Am. Chem. Soc.* **2003**, 125 (15), 4408–4409. <https://doi.org/10.1021/ja028694u>.
- (43) Hauck, D.; Jumde, V. R.; Crawford, C. J.; Titz, A. Optimized Henry Reaction Conditions for the Synthesis of an L-Fucose C-Glycosyl Derivative. In *Carbohydrate Chemistry*; 2021; pp 17–22. <https://doi.org/10.1201/9781351256087-3>.
- (44) Perret, S.; Sabin, C.; Dumon, C.; Pokorná, M.; Gautier, C.; Galanina, O.; Ilia, S.; Bovin, N.; Nicaise, M.; Desmadril, M.; Gilboa-Garber, N.; Wimmerová, M.; Mitchell, E. P.; Imberty, A. Structural Basis for the Interaction between Human Milk Oligosaccharides and the Bacterial Lectin PA-IIL of *Pseudomonas Aeruginosa*. *Biochem. J.* **2005**, 389 (2), 325–332. <https://doi.org/10.1042/BJ20050079>.
- (45) Andreini, M.; Anderluh, M.; Audfray, A.; Bernardi, A.; Imberty, A. Monovalent and Bivalent N-Fucosyl Amides as High Affinity Ligands for *Pseudomonas Aeruginosa* PA-IIL Lectin. *Carbohydr. Res.* **2010**, 345 (10), 1400–1407. <https://doi.org/10.1016/j.carres.2010.03.012>.
- (46) Šulák, O.; Cioci, G.; Lameignère, E.; Balloy, V.; Round, A.; Gutsche, I.; Malinovská, L.; Chignard, M.; Kosma, P.; Aubert, D. F.; Marolda, C. L.; Valvano, M. A.; Wimmerová, M.; Imberty, A. Burkholderia Cenocepacia Bc2l-c Is a Super Lectin with Dual Specificity and Proinflammatory Activity. *PLoS Pathog.* **2011**, 7 (9), e1002238. <https://doi.org/10.1371/journal.ppat.1002238>.
- (47) Bermeo Malo, R. Conception, Synthèse et Évaluation de Glycocomposés Dirigés Contre BC2L-C, Université Grenoble Alpes, 2021.
- (48) Morris, G. M.; Ruth, H.; Lindstrom, W.; Sanner, M. F.; Belew, R. K.; Goodsell, D. S.; Olson, A. J. Software News and Updates AutoDock4 and AutoDockTools4: Automated Docking with Selective Receptor Flexibility. *J. Comput. Chem.* **2009**, 30 (16), 2785–2791. <https://doi.org/10.1002/jcc.21256>.
- (49) Weininger, D. SMILES, a Chemical Language and Information System: 1: Introduction to Methodology and Encoding Rules. *J. Chem. Inf. Comput. Sci.* **1988**, 28 (1), 31–36. <https://doi.org/10.1021/ci00057a005>.
- (50) Korb, O.; Stützle, T.; Exner, T. E. PLANTS: Application of Ant Colony Optimization to

Structure-Based Drug Design. *Lect. Notes Comput. Sci. (including Subser. Lect. Notes Artif. Intell. Lect. Notes Bioinformatics)* **2006**, 4150, 247–258. https://doi.org/10.1007/11839088_22.

- (51) Mitchell, E. P.; Sabin, C.; Šnajdrová, L.; Pokorná, M.; Perret, S.; Gautier, C.; Hofr, C.; Gilboa-Garber, N.; Koča, J.; Wimmerová, M.; Imberty, A. High Affinity Fucose Binding of *Pseudomonas Aeruginosa* Lectin PA-III: 1.0 Å Resolution Crystal Structure of the Complex Combined with Thermodynamics and Computational Chemistry Approaches. *Proteins Struct. Funct. Genet.* **2005**, 58 (3), 735–746. <https://doi.org/10.1002/prot.20330>.
- (52) Gasteiger, E.; Gattiker, A.; Hoogland, C.; Ivanyi, I.; Appel, R. D.; Bairoch, A. ExPASy: The Proteomics Server for in-Depth Protein Knowledge and Analysis. *Nucleic Acids Res.* **2003**, 31 (13), 3784–3788. <https://doi.org/10.1093/nar/gkg563>.
- (53) Kabsch, W. XDS. *Acta Crystallogr. Sect. D Biol. Crystallogr.* **2010**, 66 (2), 125–132. <https://doi.org/10.1107/S0907444909047337>.
- (54) leggrandp; Aishima, J.; CV-GPhL. Leggrandp/Xdsme: Version Working with XDS Version: June 1, 2017 and Previous. **2017**. <https://doi.org/10.5281/ZENODO.837886>.
- (55) Winn, M. D.; Ballard, C. C.; Cowtan, K. D.; Dodson, E. J.; Emsley, P.; Evans, P. R.; Keegan, R. M.; Krissinel, E. B.; Leslie, A. G. W.; McCoy, A.; McNicholas, S. J.; Murshudov, G. N.; Pannu, N. S.; Potterton, E. A.; Powell, H. R.; Read, R. J.; Vagin, A.; Wilson, K. S. Overview of the CCP4 Suite and Current Developments. *Acta Crystallogr. Sect. D Biol. Crystallogr.* **2011**, 67 (4), 235–242. <https://doi.org/10.1107/S0907444910045749>.
- (56) McCoy, A. J.; Grosse-Kunstleve, R. W.; Adams, P. D.; Winn, M. D.; Storoni, L. C.; Read, R. J. Phaser Crystallographic Software. *J. Appl. Crystallogr.* **2007**, 40 (4), 658–674. <https://doi.org/10.1107/S0021889807021206>.
- (57) Murshudov, G. N.; Skubák, P.; Lebedev, A. A.; Pannu, N. S.; Steiner, R. A.; Nicholls, R. A.; Winn, M. D.; Long, F.; Vagin, A. A. REFMAC5 for the Refinement of Macromolecular Crystal Structures. *Acta Crystallogr. Sect. D Biol. Crystallogr.* **2011**, 67 (4), 355–367. <https://doi.org/10.1107/S0907444911001314>.
- (58) Emsley, P.; Lohkamp, B.; Scott, W. G.; Cowtan, K. Features and Development of Coot. *Acta Crystallogr. Sect. D Biol. Crystallogr.* **2010**, 66 (4), 486–501. <https://doi.org/10.1107/S0907444910007493>.